Environ. Sci. Technol. **2004**, *38,* 2413−2423

Uncertainty in Particle Number Modal Analysis during Transient Operation of Compressed Natural Gas, Diesel, and Trap-Equipped Diesel Transit Buses

BRITT A. HOLMÉN* AND YINGGE QU

Environmental Engineering Program and Civil and Environmental Engineering, The University of Connecticut, 261 Glenbrook Road, Unit 2037, Storrs, Connecticut 06269-2037

The relationships between transient vehicle operation and ultrafine particle emissions are not well-known, especially for low-emission alternative bus technologies such as compressed natural gas (CNG) and diesel buses equipped with particulate filters/traps (TRAP). In this study, real-time particle number concentrations measured on a nominal 5 s average basis using an electrical low pressure impactor (ELPI) for these two bus technologies are compared to that of a baseline catalyst-equipped diesel bus operated on ultralow sulfur fuel (BASE) using dynamometer testing. Particle emissions were consistently 2 orders of magnitude lower for the CNG and TRAP compared to BASE on all driving cycles. Time-resolved total particle numbers were examined in terms of sampling factors identified as affecting the ability of ELPI to quantify the particulate matter number emissions for low-emitting vehicles such as CNG and TRAP as a function of vehicle driving mode. Key factors were instrument sensitivity and dilution ratio, alignment of particle and vehicle operating data, sampling train background particles, and cycle-to-cycle variability due to vehicle, engine, after-treatment, or driver behavior. In-cycle variability on the central business district (CBD) cycle was highest for the TRAP configuration, but this could not be attributed to the ELPI sensitivity issues observed for TRAP-IDLE measurements. Elevated TRAP emissions coincided with low exhaust temperature, suggesting on-road real-world particulate filter performance can be evaluated by monitoring exhaust temperature. Nonunique particle emission maps indicate that measures other than vehicle speed and acceleration are necessary to model disaggregated real-time particle emissions. Further testing on a wide variety of test cycles is needed to evaluate the relative importance of the time history of vehicle operation and the hysteresis of the sampling train/dilution tunnel on ultrafine particle emissions. Future studies should monitor particle emissions with high-resolution real-time instruments and account for the operating regime of the vehicle using time-series analysis to develop predictive number emissions models.

* Corresponding author phone: (860) 486-3941; fax: (860) 486-2298; e-mail: baholmen@engr.uconn.edu.

Introduction

The increasing use of diesel particulate filter aftertreatment, ultralow sulfur diesel fuel, and compressed natural gas engines for transit buses in urban areas is a response to increasingly stringent emissions standards developed because conventional diesel vehicle exhaust has been linked to serious adverse health effects as indicated by its status as a toxic air contaminant (*1*, *2*). Ultrafine particles (diameter <100 nm) and nanoparticles (<50 nm) in vehicle exhaust may be key agents associated with elevated mortality and morbidity statistics in urban centers (*3*, *4*). Because transit buses are important sources of heavy-duty vehicle miles traveled (VMT) in urban areas, it is essential to quantify how engine and fuel type and aftertreatment technology affect ultrafine particulate matter (PM) emissions, especially under the transient driving conditions experienced in the real world.

A number of recent studies have examined the mass- and number-weighted particulate emissions from diesel engines and vehicles, chiefly using laboratory tests under *steady-state* vehicle or engine operation. Understanding the exhaust particle size distributions and how the measured distributions are affected by exhaust sampling methodology (*5*−*8*), engine type and operation (*9*−*11*), and aftertreatment technology (*12*, *13*) are important for controlling diesel vehicle emissions, implementing new engine and aftertreatment technologies, and ultimately improving urban air quality. However, there remains little fundamental data on the relationships between vehicle operating mode (cruise, idle, acceleration, deceleration) and ultrafine particle emissions, both for diesel and especially for diesel alternatives. This is due to the difficulty and expense of accurately sampling ultrafine particles and nanoparticles under transient driving conditions as well as the lack of suitable field-portable "real-time" instrumentation for on-board PM measurements compared to gaseous exhaust emissions where relationships to vehicle operating conditions have been the focus of recent research (*14*−*18*). Quantifying the relationships between heavy-duty vehicle driving mode and PM emissions is important for developing PM modal emission models, understanding the spatial distribution of PM emissions, and improving population exposure models based on travel behavior and transportation infrastructure. This study establishes preliminary relationships between PM emissions and driving mode for diesel and compressed natural gas transit buses and highlights the sampling and data analysis issues that must be understood for accurate measurement of real-world transient PM emissions that will enable comparison of current and emerging low-emission heavy-duty vehicles. Particulate emissions were quantified in real time using a Dekati electrical low pressure impactor (ELPI). The ELPI data were collected as part of a large multiagency effort led by the California Air Resources Board to collect emissions data from late-model transit buses powered by similar engines (*19*).

Two commercially available instruments—the ELPI (Dekati, Finland) and the SMPS (scanning mobility particle sizer, TSI, Inc., St. Paul, MN)—are widely used to measure the particle number concentrations and size distribution of submicrometer particles (*6*, *20*−*22*). Each instrument has its particular strengths and weaknesses based on its measurement technique. The SMPS instrument can count particles with high size resolution over limited ranges of particle electrical mobility diameter. The diameter range measured in a single SMPS scan depends on aerosol flow rate, differential mobility analyzer (DMA) geometry and voltage settings, condensation particle counter (CPC) specifications, and SMPS scan time, but is always within the instrument's ∼6−

10.1021/es034560k CCC: $27.50
Published on Web 03/10/2004

TABLE 1. ELPI Stage Diameter Ranges for 30 LPM Sample Flow Rate[a]

stage	$D_{a,50}$ (μm)	D_i (μm)	stage	$D_{a,50}$ (μm)	D_i (μm)
1	0.029	0.0407	8	0.98	1.2483
2	0.057	0.0759	9	1.59	1.9656
3	0.101	0.1287	10	2.43	3.0942
4	0.164	0.2029	11	3.94	5.0723
5	0.251	0.3121	12	6.53	8.1171
6	0.388	0.4944	inlet	10.09	
7	0.63	0.7857			

[a] $D_{a,50}$ = aerodynamic diameter of stage's lower cut point; D_i = geometric mean aerodynamic diameter of stage.

1000 nm diameter limits for the model used here (*13*, *22*). To obtain a size distribution, the DMA component of the SMPS is scanned through a range of voltages; this scanning operation severely limits the temporal resolution of the SMPS to greater than 30 s and usually to over 2 min to obtain undistorted particle size distributions. Therefore, the SMPS can only reliably measure particle size distributions from steady sources because sudden changes in source emissions during the scanning operation will result in artifact peaks in the SMPS distribution. The ELPI, on the other hand, can continuously count particles via electrical detection with high temporal resolution, but the ELPI has limited size resolution (29−10000 nm in 12 impactor stages; see Table 1) (*21*, *23*). Despite the differences in measurement principle and resolution between the two instruments, previous studies that have used both the ELPI and the SMPS to quantify size distributions during steady-state diesel engine operation have matched each other well in the instruments' overlapping size range (30−275 nm) (*20*, *24*, *25*).

This study examines how real-time ultrafine particle number concentrations and size distributions vary with vehicle operating parameters for three different transit bus configurations that represent current on-road engine and aftertreatment technologies for controlling exhaust particulate emissions: a baseline diesel bus operating on ultralow sulfur fuel with and without a passive diesel particulate filter (DPF) and a compressed natural gas (CNG) bus. An ELPI was used to measure real-time particulate emissions from these three bus configurations under two steady and three transient chassis dynamometer test cycles after dilution using an ejector-type mini dilution system as described previously (*13*). The ELPI data are evaluated to identify the factors affecting real-time modal PM number emission measurement for CNG and DPF-equipped buses that emit concentrations orders of magnitude lower than those from conventional diesel buses.

Experimental Methods

ELPI Sampling Protocols. A 30 LPM Dekati (Finland) ELPI measured diluted vehicle exhaust particle size distributions every 2−10 s (nominal 5 s time resolution). The ELPI consists of a corona charger, a 12-stage cascade low-pressure impactor, and a multichannel electrometer (*21*). The impactor stage aerodynamic diameter cut points ($D_{a,50}$) and geometric mean diameters (D_i) for the 30 LPM ELPI used in this study (Table 1) indicate that ultrafine particles (≤100 nm) were collected on ELPI stage 1 (29−57 nm) and stage 2 (57−101 nm).

The ELPI measures the current carried by charged particles impacting on the individual ELPI stages, and current values are converted to number concentrations by the ELPI software on the basis of the manufacturer's calibration of charger efficiency (*23*) and impactor properties (e.g., fine particle losses on upper stages due to diffusion (*26*)). For the 30 LPM ELPI used in this study, the current-to-number conversion factor, X, not accounting for fine particle losses, is given by the charger efficiency function provided by the manufacturer (Dekati, LTD):

$$X_{(D_s)}\,[\text{fA cm}^3] = PneQ = \begin{bmatrix} 29.024 D_s^{2.0995} & D_s < 0.035\ \mu\text{m} \\ 1.696 D_s^{1.291} & 0.035 < D_s < 10.00\ \mu\text{m} \end{bmatrix} \quad (1)$$

where P is the penetration efficiency (dimensionless), n is the average number of charges per particle, e is the unit of elementary charge (1.602×10^{-19} C), Q is the calibration flow rate (10 L/min), and D_s is the geometric mean Stokes diameter of the ELPI stage (μm). The uncorrected (for fine particle losses) number concentration is calculated as $N = IX^{-1}$, where I is the measured current (fA). This function is different from that for the 10 LPM ELPI instrument (*23*) and results in a calculated stage 1 "response factor" of 11.25 (particles/cm^3)/fA.

It should be noted that the ELPI software algorithms automatically report negative measured currents as 0 particles/cm^3. Therefore, instrument zeroing is critical for computing accurate particle number concentrations from the measured current data. In this study, after 1 h of instrument warm-up, all 12 ELPI channels were zeroed at all four measurement ranges (10000−400000 fA) before the beginning of each sampling day using the "ALL ZERO" command and the ELPI flush pump. To quantify ELPI noise levels, samples were collected with an HEPA filter on the ELPI inlet before and sometimes after testing for the day (see ELPI Electrometer Noise below).

Aluminum foil substrates purchased from Dekati were used for all ELPI stages, and the electrometer range setting was 10000 fA, but changed automatically when high currents were measured for the baseline diesel bus. Data were recorded using the "AVERAGE" option in the ELPIVI 3.1 (rev. 4.54) software so that each particle number concentration recorded at a certain time point (t) represents the average particle number concentration of the "x" seconds (x = time resolution) before time t. Because of the exhaust residence time in the minidiluter tunnel components, an 8 s time lag occurred between the test start and the ELPI data recording. Data were corrected for this short lag by adjustment of the ELPI time trace. Unless otherwise indicated, all data reported here are corrected for dilution ratio and ELPI electrical background noise as measured using an HEPA filter on the ELPI inlet before and sometimes after testing each day.

Test Vehicle Configurations. The choice of test buses was determined by the 2001 in-service fleet mix in Los Angeles. The only requirements were (1) "late-model" and in-use vehicles and (2) similar or equivalent engine technology on both CNG and diesel versions. Two transit buses were tested in three different engine/aftertreatment configurations: (1) a spark-ignition CNG bus certified for operation without an oxidation catalyst ("CNG"), (2) a conventional diesel bus operating on ultralow sulfur fuel with a passive DPF manufactured by Johnson-Matthey and known as a continuously regenerating trap (CRT, "TRAP"), and (3) the same diesel vehicle as in (2), but with the DPF replaced by a retrofit-kit-catalyzed muffler approved for use by the original equipment manufacturer ("BASE"). Both diesel configurations ran on ultralow sulfur emission control diesel (ECD-1; 11 ppm S content) fuel supplied by ARCO (a BP company). The CNG bus was powered by a diesel engine modified to operate on natural gas. All three vehicle configurations were New Flyer chassis transit buses equipped with Detroit Diesel model series 50 engines (8.5 L, four cylinders, four stroke), and vehicle mileage ranged from 15000 to 19600 prior to testing.

Dynamometer Testing. Chassis dynamometer tests were conducted at the California Air Resources Board (CARB)

TABLE 2. Test Cycle Durations and Measured Vehicle Parameters

test cycle	test period (min)	min/max speed (mph)	min/max accel (mph/s)
IDLE	35	0/0	0/0
SS55	35	54.9/56.9	−0.29/0.25
CBD	9.33	0/21.5	−8.9/4.8
NYB	10	0/31.2	−5.33/6.67
UDDS	18	0/58.8	−6.88/6.96, BASE[a] −4.51/5.8, CNG, TRAP

[a] Only one BASE-UDDS cycle of available data.

heavy-duty vehicle (HDV) emissions testing laboratory located at the Los Angeles County Metropolitan Transit Authority (MTA). The three transit bus configurations were tested on five driving cycles (Table 2); these cycles have been described in detail in previous reports (*27*, *28*). The five driving cycles were idle, steady-state cruise at 55 mph (SS55), central business district (CBD), New York bus (NYB), and urban dynamometer driving schedule (UDDS). The tests reported here were conducted from March to May 2001. Replicate test cycles were run consecutively for the relatively low emission alternative buses (CNG and TRAP) to generate sufficient mass for chemical analyses. All vehicles were preconditioned under a 50−55 mph steady-state "warm-up" for 15 min before each test sequence. Each test series was accompanied by periods of idle before and after the test; data for these idle periods were used to assess the background electrical drift of the ELPI, but no significant drift was observed before and after a test sequence.

Dilution Ratio. To date, there is little consensus on the best laboratory methodology for capturing vehicle exhaust ultrafine particle and nanoparticle size distributions that mimic real-world dilution processes, despite the documented creation of artifacts under EPA-certified dilution testing (*29*). Recognizing these limitations, the use of constant dilution ratio sampling systems, such as the ejector-type minidiluter employed by Kittelson and colleagues (*5*, *6*), allows comparisons to be made between vehicle types, especially when they are operated under transient driving conditions. Vehicle exhaust was diluted with hydrocarbon-free (activated carbon), dry (silica gel) compressed air in a single-stage, ejector-type mini dilution system (see details in ref *13*). The dilution ratio depended on the diameter of the Ni-foil inlet-restricting orifice used in the sample inlet probe. All of the tests used the dilution ratio of 64, except for additional CBD and NYB cycles on the TRAP bus that were collected on May 11 at a dilution ratio of 18.

Ancillary Data. Second-by-second temperatures of raw and dilute vehicle exhaust were measured with type K thermocouples (*13*). In addition, vehicle speed was recorded by the dynamometer software at 2 Hz resolution. A TSI model 3936 SMPS was simultaneously measuring particle size distributions at the same sampling point as the ELPI, and results have been reported previously (see ref *13* for details).

Data Analysis. The raw ELPI current data were converted to particle number counts on each stage using the correction factors for corona charger efficiency, fine particle losses, and inlet trap efficiency supplied by the manufacturer using ELPIVI software (version 3.1, rev. 4.54). Reported data are summarized by the average total number concentrations (over all 12 stages) or the size distributions for data collected over multiple tests on any given driving cycle.

Particle Size Distributions (dN/(d log Dp)). ELPI data were recorded as the number-weighted particle concentration (dN) for each stage (number of particles/cm^3). After normalization by d log Dp (d log Dp_i = log $D_{a,50,i+1}$ − log $D_{a,50,i}$) of each stage i, the ELPI raw data were converted to normalized particle number concentrations (dN/(d log Dp)) for plotting particle number size distributions. Because multiple repetitions of each test cycle were measured (see Table 3), the average and standard deviation of the particle number concentration for each ELPI stage were calculated using the test data collected over all individual tests of each test cycle.

TABLE 3. Number of Individual Tests of Each Test Cycle

vehicle configuration	CBD	NYB	UDDS	SS55	IDLE	total
BASE	8	3	4	2	2	19
TRAP	21	18	12	3	2	56
CNG	18	16	6	2	2	44

Average Particle Number Concentrations (number of particles/cm^3). The number of ELPI data points measured for individual test cycles ranged from 120 to 1000, depending on the recorded ELPI time resolution and overall length of the driving cycle (~10−35 min). The particle counts on each ELPI stage were averaged over each individual test cycle to give the average particle number concentration for a given driving cycle test. In addition, total particle number concentration (TPN) was calculated by summing the concentration measured in each of the 12 stages for each ELPI measurement. These TPN values were summed over the time duration of an individual test cycle to determine the cycle TPN and the cycle TPN divided by the number of measurements during the cycle to compute the *average TPN* for a given cycle.

Speed, Acceleration, and Particle Number Concentration Maps. To examine particle number concentration relationships with vehicle driving mode (cruise, acceleration, deceleration, idle) during transient operation, color map plots of speed, acceleration, and particle number concentration were generated. First, second-by-second acceleration was calculated from the raw vehicle speed data (recorded every ~0.5 s by the dynamometer software). The raw speed data were corrected for the time lag between vehicle operation and ELPI sampling of vehicle exhaust, and then the speed and acceleration data were averaged to correspond to the recorded ELPI data points. There were no vehicle speed data for the CNG bus on the NYB cycle (CNG-NYB) or for more than one BASE test on the UDDS cycle (BASE-UDDS) due to data recording errors. Therefore, modal comparisons between the three bus configurations are conducted using only the CBD cycle tests.

The sums of the particle concentrations over all 12 ELPI stages at each time point, or "instantaneous TPN", were compared for the three bus configurations on the CBD cycle as this cycle had multiple test data for speed and number concentration for all three vehicle configurations. The 560 s, 3.2 km CBD cycle has 14 repetitions of (i) 7 s of idle, (ii) 10 s of acceleration to 20 mph, (iii) 20 mph cruise for 18.5 s, and (iv) 4.5 s of deceleration to idle. Test variability, quantified as the coefficient of variation (CV = the ratio of the standard deviation to the mean, reported as percent), was assessed for average total particle number concentrations by averaging over individual data points in all the CBD cycle measurements for a given bus configuration.

Results and Discussion

Total Number Concentrations. Testing of each bus involved running different numbers of individual tests on each cycle (Table 3) to obtain sufficient total PM mass for chemical analysis by other researchers (see ref *28*). Over 90% of the total particle number concentrations over all five test cycles were measured in ELPI stages 1−3 (29−164 nm), and ultrafine particles (<100 nm or ELPI stages 1 and 2) comprised more

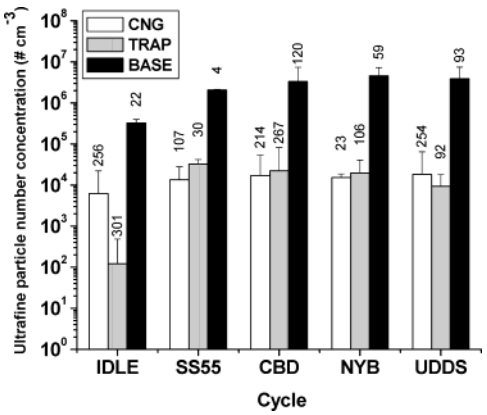

FIGURE 1. Average ultrafine particle number concentrations on all replicates of five test cycles for the three bus configurations. Ultrafine particles are defined as the sum of ELPI stages 1 and 2. The error bars indicate 1 standard deviation of the mean concentrations, and labels on each bar represent the coefficient of variation (%).

than 60% of the total particle number concentration measured by the ELPI for all three bus configurations. As expected, for all five driving cycles the total average ultrafine particle number concentrations from the baseline diesel bus outfitted with an oxidation catalyst (BASE) were more than 100 times higher than those measured for the two alternative bus configurations (CNG and TRAP) (Figure 1). This result agrees with our previous measurements using an SMPS to quantify 6−237 nm particles on steady-state cycles (*13*). Idle operation always resulted in the lowest average ultrafine particle number concentrations compared to the other test cycles for all bus configurations (Figure 1). Figure 1 also shows that average CNG ultrafine emissions were low and similar on all five cycles whereas the TRAP-IDLE 29−101 nm emissions were significantly lower than those of the other four cycles. As will be discussed in more detail below (see Uncertainty), the TRAP-IDLE emissions collected at a dilution ratio (DR) of 64 were also highly variable as indicated by the CV labels on each bar in Figure 1. Possible causes of this variability are (i) inherent variability in the operation of the CRT filter as a function of exhaust and engine operation properties and (ii) measurement uncertainty when concentrations close to the ELPI's detection limit are measured at the dilution ratio (DR = 64) used in this study.

Particle Size Distributions. The baseline diesel (BASE) bus had significantly higher ELPI particle counts than the CNG and TRAP buses over the entire diameter range measured for both steady (IDLE, SS55) and transient (CBD, NYB, UDDS) operation (Figure 2). Under higher load conditions (SS55, CBD, NYB, UDDS), the TRAP and CNG emissions were similar over the entire submicrometer size range for the CBD cycle and over ELPI stages 1−4 for SS55, NYB, and UDDS (Figure 2). It is interesting to note that the TRAP bus had essentially undetectable particle counts after correction for HEPA blanks on ELPI stages 6−12 ($D_p \approx >300$ nm) during steady-state 55 mph operation, whereas CNG counts were significant (Figure 2, SS55). Thus, the TRAP removed all particles of >300 nm during high-load steady-state operation (SS55). Note, however, that on the transient cycles (CBD, NYB, UDDS) the TRAP counts were detectable on stages > 6.

There were also differences in the particle number distributions between the two low-emission buses, CNG and TRAP, under idle conditions at DR = 64. Most notably, the CNG bus had considerably higher (more than a factor of 10) ELPI stage 1 and stage 2 (D_p < 101 nm) number concentrations than the TRAP bus under idle operation (Figure 2, IDLE).

Real-Time Transient Cycle Total Number Concentrations. The advantage of the ELPI instrument is that real-time

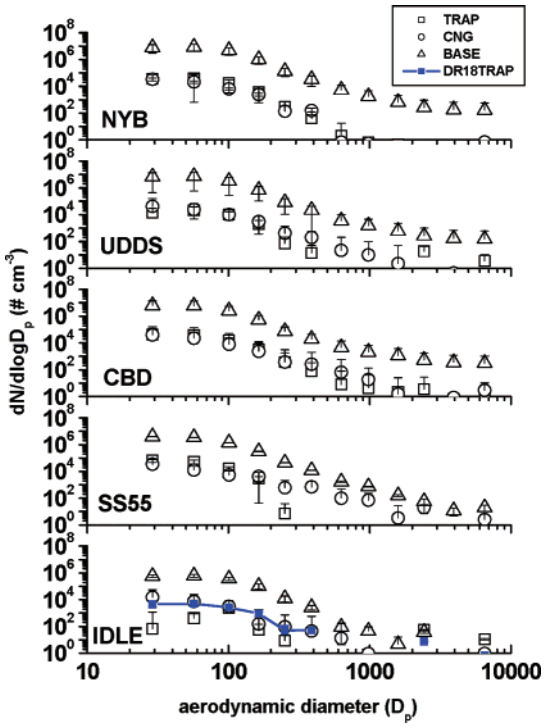

FIGURE 2. ELPI particle size distributions on three transient cycles (NYB, UDDS, CBD) and two steady cycles (SS55, IDLE) for each bus configuration. The scale of the *y*-axis is the same for the five plots (10^0 to 10^8 cm^{-3}). Error bars indicate 1 standard deviation over replicate test cycles. The IDLE plot includes data for TRAP collected under a dilution ratio of 18 (blue line).

particle size distributions can be measured at temporal resolutions as low as 2 s (*21*), thus allowing monitoring of transient driving cycle emissions. In practice, the ELPI data were recorded as 2−10 s (nominally 5 s) averages (determined by laptop capabilities), and vehicle speed data were averaged over the same time intervals to determine relationships among TPN, speed, and acceleration. Averaging the ELPI data over times longer than the stage residence times (0.0057−0.0467 s in 30 LPM ELPI) avoids the induced current (or image charge) signal created when very fast concentration changes are sampled. The regular sawtooth pattern of the CBD cycle (see Figure 3b) was used to examine differences between the three bus configurations. The raw (uncorrected for HEPA and dilution) ELPI total particle number concentrations on a nominal 5 s average basis (Figure 3a,c,e) together with the corresponding average measured CBD cycle vehicle speed traces (Figure 3b,d,f) as a function of time in the cycle indicate how the number concentration varied within the CBD cycle and between individual bus-cycle tests.

The BASE-CBD TPN-vs-time traces were the most reproducible from test to test (Figure 3a), followed by TRAP (Figure 3c), and the CNG bus had number concentration time-series plots that were relatively irregular (Figure 3e) compared to the diesel bus configurations. The CNG speed−time traces (Figures 3f) were also more variable between tests than for the diesel vehicles (Figure 3b,d), and may have contributed variability to the ELPI data (Figure 3e) due to difficulty in aligning individual CNG-CBD cycles. The apparent higher variability for CNG and TRAP compared to BASE reflects the fact that additional factors affect real-time measurement of PM emissions when absolute particle concentrations are low, as for CNG and TRAP.

Uncertainty in ELPI Measurement of Exhaust Particle Number Concentrations. Accurate time-resolved ELPI particle number concentration measurements during transient vehicle operation depend on instrument factors (ELPI

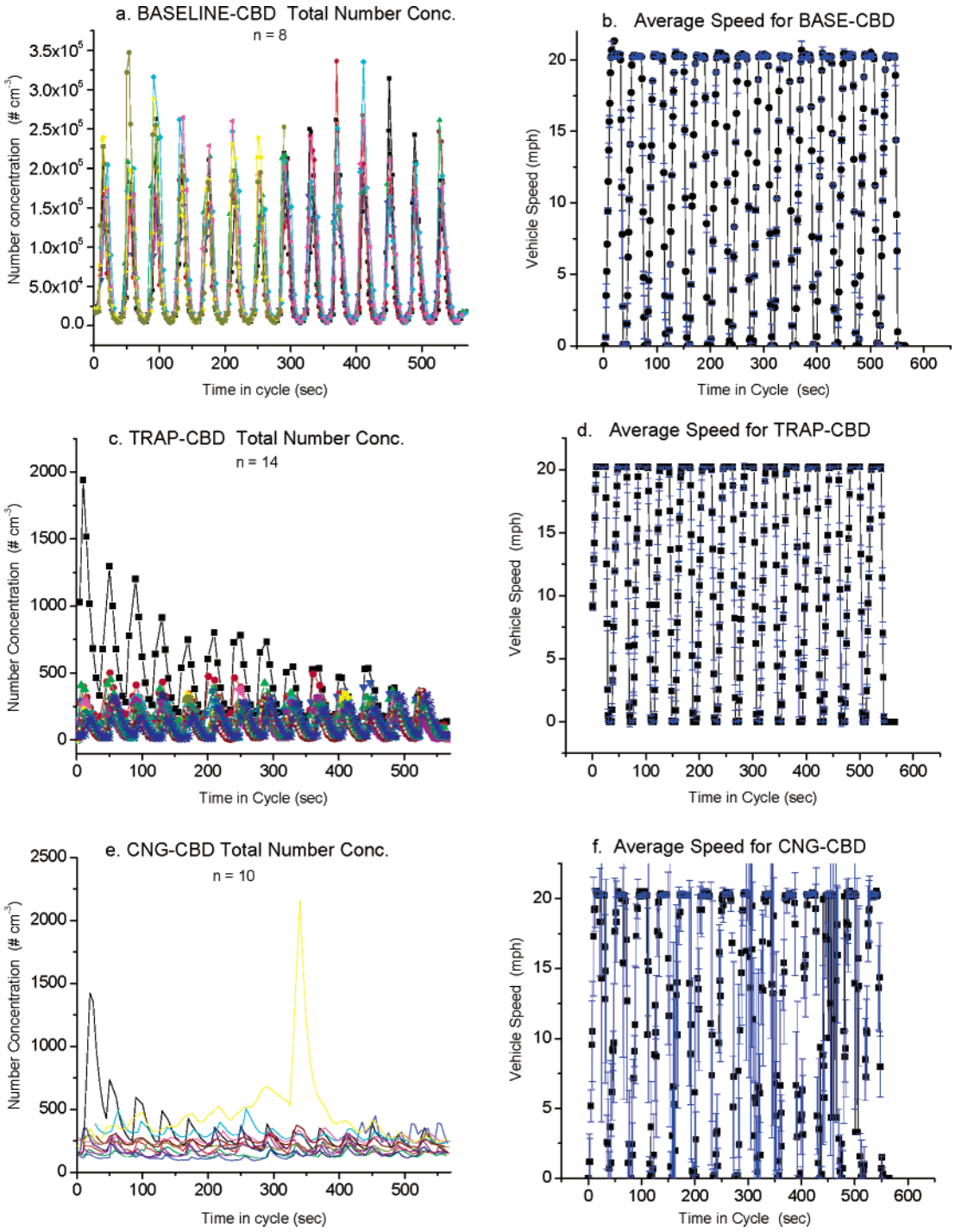

FIGURE 3. Raw total particle number concentrations (uncorrected for dilution and HEPA background) and speed traces for individual CBD cycles averaged over ~5 s resolution for (a, b) BASELINE, (c, d) TRAP, and (e, f) CNG bus configurations. *n* = number of CBD cycles.

electrometer noise and instrument zeroing, ELPI charger efficiency and impactor fine particle loss correction) as well as external factors including exhaust dilution ratio, which determines the raw concentration measured by the ELPI. For low-emission vehicles such as the CNG and TRAP buses, particular attention must be paid to "background" (dilution air, dilution tunnel) particle concentrations because under some operating conditions the exhaust concentrations may be near ambient levels. These factors and the experimental approach needed to evaluate the magnitude of each factor are summarized in Table 4.

ELPI Electrometer Noise. The HEPA measurement response currents ranged from a minimum reading of −7 fA (May 10, TRAP bus) to a maximum value of +7 fA (Mar 21, CNG bus) over the entire 3-month sampling period, and HEPA daily averages were between −5 and +1 fA for stages 1−3 (see Figure 4a). Corresponding particle number concentrations from HEPA measurements on stages 1−3 were less than 15 particles per cubic centimeter (Figure 4b). Over 90% of all HEPA measurements were within the range of −5 to +2 fA. The noise levels observed using the 30 LPM ELPI instrument during individual driving cycle tests were much lower than the daily averages, only 1−2 fA. Therefore, estimated lower quantifiable limits for the 30 LPM ELPI due to instrument noise during a driving cycle were ~27 particles/cm^3 on stage 1, ~12 particles/cm^3 on stage 2, and ~6 particles/

TABLE 4. Causes of Uncertainty in ELPI Modal Particle Number Measurement

factor affecting ability to quantify *N*	experimental approach	type[a]
ELPI electrometer noise and zeroing	collect HEPA data	I
impactor losses (diffusion, evaporation, etc.)	Dekati calibration/correction	I
ELPI sampling rate/averaging	collect data at different Δt values	I, S
sampling train artifacts/hysteresis	collect tunnel blanks	S
background particle concentrations	collect tunnel blanks	S
exhaust DR	vary DR and compare *N*	S
alignment of engine/vehicle operation and emissions data	synchronize clocks, measure lag	S
variation in vehicle operation (backfires, DPF operation)	collect ancillary data	V
test-to-test inherent variability	collect replicate test cycles	V, I, S

[a] I = instrument; S = sampling setup; V = vehicle (engine, aftertreatment, driver).

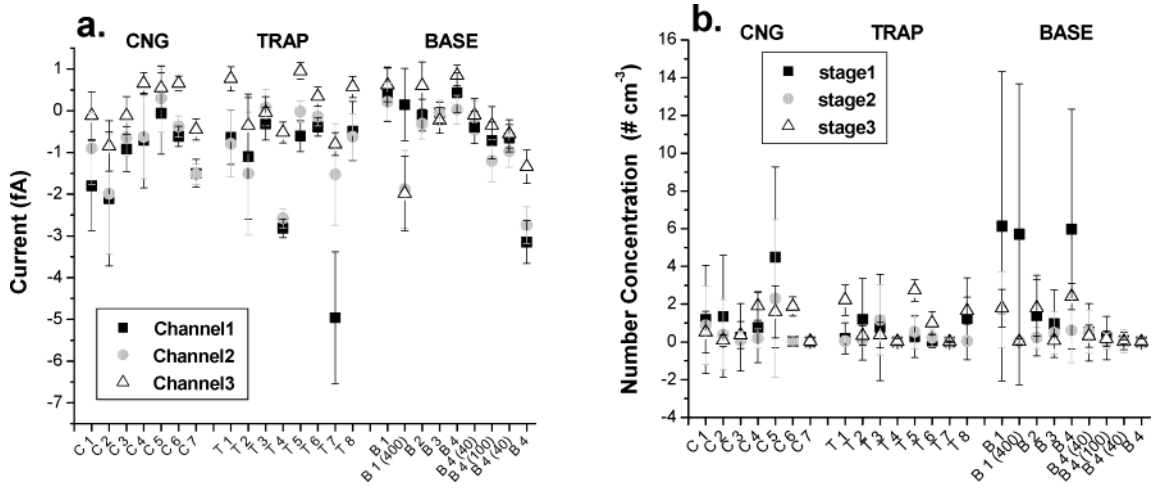

FIGURE 4. Daily mean and standard deviation of ELPI noise measurements made with an HEPA filter on the ELPI inlet: (a) Current for channels 1−3 and (b) corresponding number concentrations for stages 1−3. The *x*-axis indicates the day of sampling a given bus configuration (C = CNG, T = TRAP, B = BASE), and for BASE, the value in parentheses is the electrometer range (pA) when HEPA data were collected at a range other than 10000 fA.

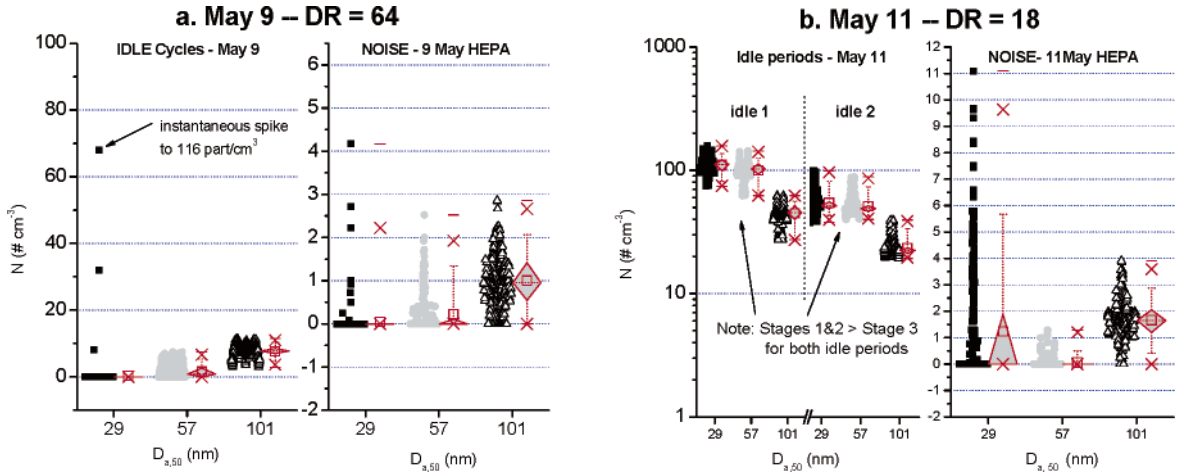

FIGURE 5. Box plots of TRAP-IDLE and daily HEPA measurements on (a) May 9 (DR = 64) and (b) May 11 (DR = 18). Individual raw particle number concentrations (*N*) are shown by filled symbols for ELPI stages 1−3. Box plots to the right of the symbols show the mean (open square), 1% and 99% (X), 5% and 95% (shaded tilted square), and minimum and maximum (−) values.

cm^3 on stage 3. As discussed in more detail below, raw (before DR correction) particle number concentrations of this magnitude were measured only during idle operation of the TRAP bus.

Idle Emissions for Low-Emission Vehicles and ELPI Sensitivity. The high CV for TRAP-IDLE in Figure 1 and very low stage 1 and stage 2 TRAP-IDLE counts in the size distributions (Figure 2) may have been due to ELPI sensitivity issues at DR = 64. The dilution ratio of 64 was selected (1) so that one dilution ratio could be used for all vehicles to avoid differences in particle formation within the sampling train and (2) to avoid potential particle nucleation artifacts associated with small dilution ratios (*5*). The dilution ratio was lowered to 18 on May 11 for some replicate CBD and NYB cycle tests. Data from May 11 were used to evaluate the effect of dilution ratio on ELPI sensitivity. As shown in Figure 5, the ELPI HEPA noise measurements were comparable for May 9 (DR = 64) and May 11 (DR = 18), indicating that the ELPI zeroing levels were comparable on these days. Data for IDLE operation on both days, however, were quite different

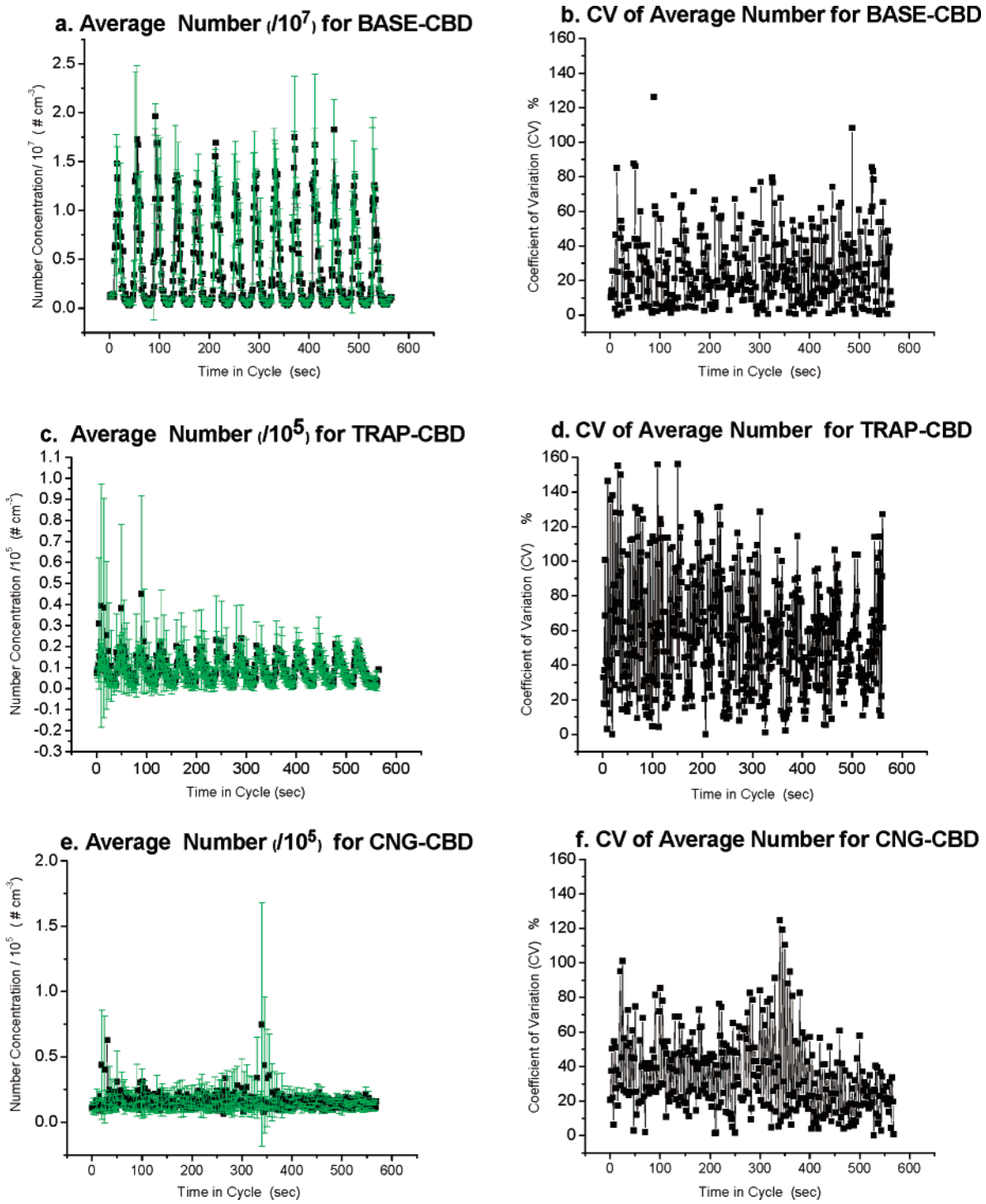

FIGURE 6. Average total ELPI number concentration (left panels) and CV (right panels) on a 5 s basis in the CBD cycle for three bus configurations: baseline diesel, trap-equipped diesel, and CNG. Averages are based on 8, 14, and 10 repetitions of the CBD cycle for BASE, TRAP, and CNG, respectively. Note that *y*-axis number concentration scales are normalized to 10^5 (TRAP and CNG) or 10^7 (BASE) particles/cm^3 and CV plots have identical *y*-axis scales. CV was computed as ((standard deviation)/mean) × 100 for each time point over all CBD test cycles for each bus.

(Figure 5). At the lower dilution ratio, two periods of bus idling had raw number concentrations on stages 1−3 of 20−200 particles/cm^3, and the size distribution trend was stage 1 ≈ stage 2 > stage 3 (Figure 5b). In contrast, ELPI measurements of IDLE operation at DR = 64 (May 9, Figure 5a) show that the majority of stage 1 IDLE concentrations were zero and the pattern of the means was stage 1 < stage 2 < stage 3. Comparison of the TRAP-IDLE cycle size distribution plots at the two dilution ratios (Figure 2, IDLE) shows that the TRAP-IDLE distribution at DR = 18 (Figure 2, DR18TRAP line in IDLE plot) was similar to the CNG bus IDLE distribution and had much higher confidence on each ELPI stage compared to the DR = 64 TRAP-IDLE distribution. *Therefore, at DR = 64, the ELPI was not able to accurately quantify the IDLE emissions from the TRAP vehicle because the raw particle concentrations were near the instrument's detection limit.* In contrast, CNG-IDLE emissions were readily quantifiable at DR = 64, and mean CNG-IDLE raw ultrafine particle counts exceeded HEPA noise by a factor of at least 10.

Idle operation is common for heavy-duty diesel vehicles and may comprise 40% of vehicle operating time (*30*); therefore, understanding differences in idle emissions between alternative heavy-duty vehicle types is important for setting emissions control policy and selecting the transit bus technology that will best improve air quality under all vehicle operating conditions. The ELPI data indicate that, on average, diesel DPF aftertreatment may be more effective at reducing idle emissions of the smallest ultrafine particles measured by ELPI (29−57 nm) than running CNG buses certified to operate without oxidation catalysts. Furthermore, for accurate low-emission vehicle particle concentration measurements, selection of dilution ratio requires delicate balancing between instrument sensitivity issues and possible nanoparticle formation artifacts due to sampling conditions that do not mimic real-world dilution conditions.

These results indicate that (1) repeated HEPA measurements should be performed intermittently over the course of a sampling day to both allow the best estimates of electrometer noise for individual test cycles and account for electrometer drift over long sampling durations and (2) except for idle operation of the TRAP bus, the 30 LPM ELPI accurately quantified number emissions at a dilution ratio of 64. Considering that all driving cycles include periods of idle, overall cycle uncertainty may be a function of the fraction of idle time in a cycle, especially when emissions from low-emission vehicles such as TRAP are quantified, but this was not confirmed in this study.

Test-to-Test Variability. To quantitatively compare the overall variability at individual time points in the CBD cycle for each vehicle, the mean number concentration was computed by averaging across all the individual tests shown in Figure 3 and computing the standard deviation for each time point in the cycle. As shown in Figure 6a,c,e, the number concentration standard deviations computed at each time point in the CBD cycle were consistently highest at the peaks in the number concentration time trace for BASE and at early times in the cycle for TRAP-CBD. For the CNG vehicle, the highest standard deviation occurred near midcycle (at about 340 s in Figure 6e) due to a large spike during a single test (see Figure 3e). The CV at each time point was computed to allow comparison between vehicles (Figure 6b,d,f). The TRAP configuration had consistently high CV values and also had the highest range of CV (up to 160%), compared to BASE and CNG. The higher variability for the TRAP vehicle compared to CNG cannot be attributed to measurement variability when concentrations are close to the ELPI's detection limit because the CNG particle number concentrations were typically lower than those from the TRAP bus. In addition, no relationship was found between measurement variability and speed, as one would expect if the TRAP-CBD cycle high variability was due to the idle parts of the CBD cycle. Therefore, the high TRAP CV values in Figure 6 compared to those of BASE and CNG suggest that the diesel particulate filter contributed to variability in particle emissions. In contrast, the CNG vehicle displayed isolated CBD tests where spikes of elevated particle emissions occurred (Figure 3e) and also routinely showed isolated peaks in ultrafine emissions during idle operation (data not shown), suggesting intermittent engine backfire. Such instantaneous PM spikes from spark-ignition engines have been reported previously (*8*, *31*, *32*), and particulate emissions from diesel engines are known to be more consistent than those from spark-ignition engines (*8*).

Aftertreatment Effects. The TRAP-CBD tests were driven as four back-to-back individual cycles, and it was observed that the first test in the series of four had elevated particle number concentrations relative to the other three tests; this was most pronounced for the first test of the day (see Figure 3c, black squares). In addition, over the first test period there

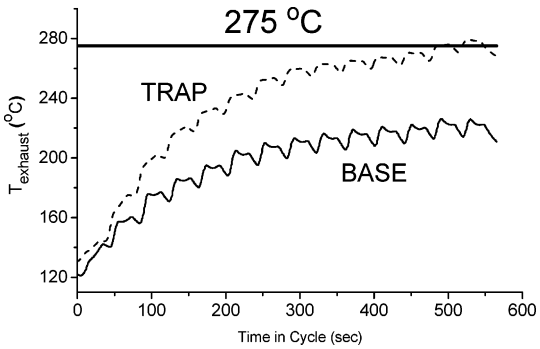

FIGURE 7. Comparison of exhaust temperatures for TRAP and BASE diesel vehicle configurations on the first CBD cycle in a sequence of back-to-back tests.

was a decreasing trend in ELPI number concentration down to a stable level that was then measured reproducibly on the following replicate tests. The elevated counts on the first test in a sequence occurred despite the 15 min warm-up (steady-state 55 mph) period prior to every first test in a sequence. Elevated particle emissions on the first test were not observed for the BASE configuration, suggesting that the particle filter played a role in the elevated emissions observed at the beginning of this sequence. To investigate the differences between the TRAP and BASE vehicle emissions further, the exhaust temperature data were examined in more detail for the first CBD test in a sequence (Figure 7). The CRT filter uses NO_2 to oxidize the particles that are captured by the filter. This reaction requires exhaust temperatures >275 °C over 40−50% of the duty cycle to maintain optimum CRT performance (*12*, *33*, *34*). There was only one TRAP-CBD test that had exceedingly high particle emissions (Figure 3c, black squares), and this test also had the lowest average exhaust temperature of all the CBD-TRAP tests ($T \approx 232$ °C compared to $T > 263$ °C for all other TRAP-CBD tests). Thus, the relatively high particle number emissions may have occurred because the CRT filter was not operating optimally during this test and semivolatile species formed nanoparticles downstream of the CRT while exhaust temperature was low.

The occurrence of elevated ultrafine particle number emissions from the TRAP vehicle when operated at a lower exhaust temperature suggests that field monitoring of exhaust temperature may be useful for assessing ultrafine particle emissions variability in addition to verifying that on-road operation is actually achieving the reduced PM emissions specified for the device. These data also indicate that when the CRT is operating within the specifications required for states to claim mass-based emissions credits for particulate filter retrofits (*34*), unregulated ultrafine particle number emissions from CRT-equipped transit buses will also be effectively reduced.

Particle Emission Maps. Quantifying the particulate emissions of a vehicle as a function of vehicle operating conditions or "mode" (acceleration, deceleration, idle, and cruise) is important to both develop effective particulate emissions control technologies and predict particle emissions as a function of driver behavior. The laboratory data collected here are restricted in terms of the range of operating conditions encompassed in the individual driving cycles tested. However, preliminary comparisons between the different modes for the three vehicle configurations highlight some key relationships and point to sampling methodologies that need to be investigated further in the future. The emissions data reported here are in terms of ELPI total number concentrations (number of particles/cm^3), not emission rates (number of particles/s), which will be necessary to ultimately quantify particle flux as functions of instantaneous vehicle operating parameters. However, be-

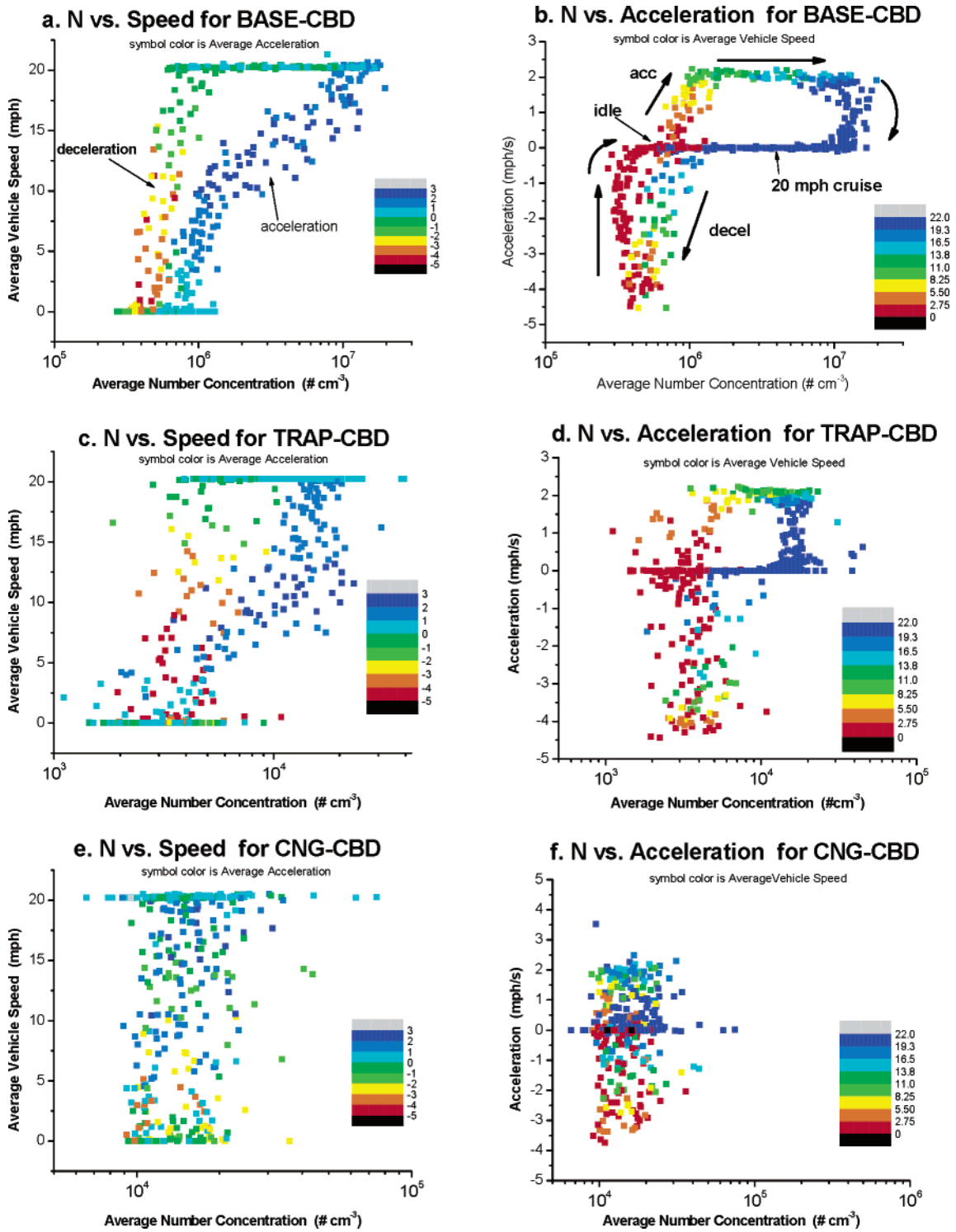

FIGURE 8. Color map plots of total particle number concentration vs vehicle speed (left panels) and acceleration (right panels) on the CBD cycle for three bus configurations. Symbol color indicates average vehicle acceleration rate, which ranges from −5 to +3 mph/s, in (a), (c), and (e). Symbol color indicates average vehicle speed in (b), (d), and (f), which ranges from 0 to 22 mph.

cause the CBD cycle is quite uniform and all three bus configurations had equivalent engine makes, sizes (four cylinders, 8.5 L), and gearing ratios (rated power 275 hp at 2100 rpm and peak torque 890 lb ft at 1200 rpm), exhaust flow rates over the CBD cycle should vary similarly and allow valid comparisons in terms of number concentration.

Figure 8 shows relationships between vehicle speed and acceleration on the CBD cycle and TPN, with the symbol colors indicating the average acceleration (left panels, Figure 8) or average vehicle speed (right panels, Figure 8). The BASE-CBD relationships clearly indicate higher particle emissions on acceleration compared to deceleration, and the positive slopes of both the acceleration and deceleration limbs of the plot show that TPN increased as speed increased for a given driving mode (acceleration or deceleration) (Figure 8a). The acceleration vs deceleration pattern is less obvious for TRAP-CBD, but as for BASE-CBD, the highest TPN occurred during acceleration events at the highest speed in the cycle (20 mph) (Figure 8c). There was no discernible relationship for CNG-CBD (Figure 8e) possibly due to the routinely variable

CNG emissions that resulted in similar magnitude TPN emissions under all driving modes in the CBD cycle. The lack of clear relationships for CNG-CBD may also have been due to the difficulty of lining up vehicle speed data with the ELPI data when number concentrations between idle and cruise operation in the CBD cycle were not very different. Field efforts made to reduce uncertainty in data alignment included daily synchronization of computer clocks, measurement of ELPI response time based on real time, not recorded ELPI data time, and honking the vehicle horn at the initiation of every driving cycle, even when driven back-to-back.

For the color maps with acceleration on the *y*-axis and symbol color indicating vehicle speed, the BASE-CBD relationships (Figure 8b) were again very distinct, and the highest number emissions occurred at the highest speeds (>16 mph). The lowest number emissions occurred during decelerations at low speed, most likely as the vehicle approached idle operation. The TRAP-CBD relationships are similar to those for BASE-CBD, but more scatter exists in the low-speed portions of the plot (Figure 8d), likely due to ELPI sensitivity issues discussed previously. Emissions for CNG-CBD encompassed the smallest range in number concentration with a range less than a factor of 10, and there was little distinction between driving mode and particle emissions from the CNG vehicle.

The data in Figure 8 suggest that parameters other than vehicle speed and acceleration are needed to predict TPN from these transit buses because different combinations of speed−acceleration resulted in the same total ultrafine particle emissions when averaging was done over ∼5 s intervals in a relatively conservative transient driving cycle. Similarly, vehicle specific power did not give unique relationships with number concentration. It is possible that there is a time dependence in particle emissions. In other words, the operating history of the vehicle over some time period longer than 5 s prior to *t* may determine the particle concentration measured at time *t*. For example, whether the vehicle arrives at a particular speed−acceleration value via acceleration or deceleration could result in two different ultrafine particle emissions values. Quantifying these relationships will depend on collecting high-resolution particle and vehicle operating data for time-series analysis. Another possibility is that hysteresis associated with the sampling train/dilution tunnel explains the lack of unique speed−acceleration−TPN relationships for these vehicles. Evaluation of this latter effect will require extensive tunnel blank testing under a range of sampling conditions.

Quantifying real-world particulate matter emissions from in-use vehicles will ultimately require on-board measurements during actual on-road driving to capture the full range of instantaneous vehicle operating modes. The following sampling concerns should be taken into consideration. First, ultrafine particle emissions need to be sampled with high enough temporal resolution to capture the transient acceleration events that produce high number concentrations. The 5 s averages used in the present study did not adequately monitor these instantaneous events, and sampling times of <1 s may be necessary. This will require implementation and detailed characterization of the new fast-response particle size distribution instruments such as the EEPS (engine electrical particle spectrometer, TSI, Inc.) and DMS-500 (Cambustion, U.K.). Use of the new ELPI electrical filter stage (*35*) that will enable real-time detection of particles down to 7 nm also needs to be investigated in detail over a wide range of operating modes. For the alternative vehicle configurations such as TRAP and CNG that have relatively low particle emissions, the lower detection limit of these new devices will be a major sampling concern. We observed a sensitivity to dilution ratio for the TRAP measurements; therefore, the tradeoffs among measured ultrafine size distributions, dilution conditions, and background particle concentrations should be carefully considered in future studies with low emission vehicles.

It is essential that vehicle operating parameters also be collected at high temporal resolution to accurately map the emissions profiles as a function of driving mode. Although no dependency on sampling rate could be identified in this study, this conclusion is restricted to the range of sampling rates used in this study (2−10 s) on the basis of comparing peak instantaneous TPN concentration over CBD cycles. The CBD peaks did not increase as the averaging period decreased; therefore, other factors associated with measuring particulate matter in diesel vehicle exhaust were more important than the ELPI sampling rate in terms of comparing the three vehicle configurations under transient driving conditions. High sampling rate will also improve the ability to align the vehicle emissions and speed data and make corrections for lags between emissions and measurement that are critical to valid data interpretation.

Acknowledgments

We thank Alberto Ayala (CARB) and Harvey Porter, Keith Stiglitz, and Fred Gonzales (CAVTC) for project management, dynamometer expertise, and assistance with the mini dilution system. The thoughtful comments of three reviewers are also appreciated. Funding was provided by the California Air Resources Board, NSF Grant BES-0132759, and the UCONN Environmental Research Institute.

Literature Cited

(1) U.S. EPA. *Code of Federal Regulations*, 40 CFR Part 80, 2001, 17230−17273.
(2) Scientific Review Panel. *Findings on The Report on Diesel Exhaust*; Sacramento, CA, 1998.
(3) Donaldson, K.; Li, X. Y.; MacNee, W. *J. Aerosol Sci.* **1998**, *29*, 553−560.
(4) Stober, W.; Mauderly, J. L. *Inhalation Toxicol.* **1994**, *6*, 427−457.
(5) Abdul-Khalek, I.; Kittelson, D.; Brear, F. *SAE Tech. Pap. Ser.* **1999**, *No. 1999-01-1142*.
(6) Abdul-Khalek, I. S.; Kittelson, D. B.; Graskow, B. R.; Wei, Q.; Brear, F. *SAE Tech. Pap. Ser.* **1998**, *No. 980525*.
(7) Maricq, M. M.; Chase, R. E.; Xu, N. *J. Air Waste Manage. Assoc.* **2001**, *51*, 1529−1537.
(8) Kayes, D.; Hochgreb, S. *SAE Tech. Pap. Ser.* **1998**, *No. 982601*.
(9) Kittelson, D. B. *J. Aerosol Sci.* **1998**, *29*, 575−588.
(10) Greenwood, S. J.; Coxon, J. E.; Biddulph, T.; Bennett, J. *SAE Tech. Pap. Ser.* **1996**, *No. 981085*.
(11) Kayes, D.; Hochgreb, S. *Environ. Sci. Technol.* **1999**, *33*, 3957−3967.
(12) Lanni, T.; Chatterjee, S.; Conway, R.; Windawi, H.; Rosenblatt, D.; Bush, C.; Lowell, D.; Evans, J.; Mclean, R. *SAE Tech. Pap. Ser.* **2001**, *No. 2001-01-0511*.
(13) Holmén, B. A.; Ayala, A. *Environ. Sci. Technol.* **2002**, *36*, 5041−5050.
(14) Barth, M.; An, F.; Younglove, T.; Scora, G.; Levine, C. *Development of a Comprehensive Modal Emissions Model: Final Report*; National Cooperative Highway Research Program (NCHRP Project 25-11), Washington, DC, 2000.
(15) Frey, H. C.; Unal, A.; Chen, J. *Recommended Strategy for On-Board Emission Data Analysis and Collection for the New Generation Model*; Office of Transportation and Air Quality, U.S. EPA: Washington, DC, 2002.
(16) Joumard, R.; Jost, P.; Hickman, J.; Hassel, D. *Sci. Total Environ.* **1995**, *169*, 167−174.
(17) Holmén, B. A.; Niemeier, D. A. *Transp. Res., Part D* **1998**, *3*, 117−128.
(18) Sturm, P. J.; Boulter, P.; de Haan, P.; Joumard, R.; Hausberger, S.; Hickman, J. A.; Keller, M.; Niederle, W.; Ntziachristos, L.; Reiter, C.; Samaras, Z.; Schinagl, G.; Schweizer, T.; Pischinger, R. *Instantaneous emission data and their use in estimating passenger car emissions*; Technical University Graz: Graz, Austria, 1998.

(19) California Air Resources Board. ARB CNG and Diesel Transit Bus Emissions Research. http://www.arb.ca.gov/research/cng-diesel/cng-diesel.htm (Oct 31, 2003).
(20) Ahlvik, P.; Ntziachristos, L.; Keskinen, J.; Virtanen, A. *SAE Tech. Pap. Ser.* **1998**, *No. 980410*.
(21) Keskinen, J.; Pietarinen, K.; Lehtimaeki, M. *J. Aerosol Sci.* **1992**, *23*, 353−360.
(22) TSI, Inc. *Model 3936-Series Scanning Mobility Particle Sizers*; St. Paul, MN, 1998.
(23) Marjamäki, M.; Keskinen, J.; Chen, D.-R.; Pui, D. Y. H. *J. Aerosol Sci.* **2000**, *31*, 249−261.
(24) Shi, J. P.; Harrison, R. M. *Environ. Sci. Technol.* **1999**, *33*, 3730−3736.
(25) Moisio, M.; Hautanen, J.; Virtanen, A.; Marjamäki, M.; Keskinen, J. *J. Aerosol Sci.* **1997**, *28* (Suppl. 1), S143−S144.
(26) Virtanen, A.; Marjamäki, M.; Ristimäki, J.; Keskinen, J. *J. Aerosol Sci.* **2001**, *32*, 389−401.
(27) Ayala, A.; Kado, N.; Okamoto, R.; Rieger, P.; Holmén, B.; Stiglitz, K. E. 12th CRC On-road Vehicle Emissions Workshop, San Diego, CA, 2002.
(28) Ayala, A.; Kado, N. Y.; Okamoto, R. A.; Holmén, B. A.; Kuzmicky, P. A.; Kobayashi, R.; Stiglitz, K. E. *SAE Tech. Pap. Ser.* **2002**, *No. 2002-01-1722*, 1−12.
(29) Maricq, M. M.; Podsiadlik, D. H.; Chase, R. E. *Environ. Sci. Technol.* **1999**, *33*, 1618−1626.
(30) Brodrick, C.-J.; Lipman, T. E.; Farshchi, M.; Lutsey, N. P.; Dwyer, H. A.; Sperling, D.; Gouse, S. W.; Harris, D. B.; Jr., F. G. K. *Transp. Res., Part D* **2002**, *7*, 303−315.
(31) Graskow, B. R.; Kittelson, D. B.; Abdul-Khalek, I. S.; Ahmadi, M. R.; Morris, J. E. *SAE Tech. Pap. Ser.* **1998**, *No. 980528*.
(32) Lanni, T.; Frank, B. P.; Tang, S.; Rosenblatt, D.; Lowell, D. *SAE Tech. Pap. Ser.* **2003**, *No. 2003-01-0300*.
(33) Johnson Matthey. CRT (Continuously Regenerating Technology) Filter. http://www.jmcsd.com/html/crt.html (2001).
(34) U.S. EPA. Voluntary Diesel Retrofit Program. http://www.epa.gov/otaq/retrofit/techlist-johnmatt.htm (May 12, 2003).
(35) Marjamäki, M.; Ntziachristos, L.; Virtanen, A.; Ristimäki, J.; Keskinen, J.; Moisio, M.; Palonen, M.; Lappi, M. *SAE Tech. Pap. Ser.* **2002**, *No. 2002-01-0055*.

Received for review June 5, 2003. Revised manuscript received January 23, 2004. Accepted January 28, 2004.

ES034560K